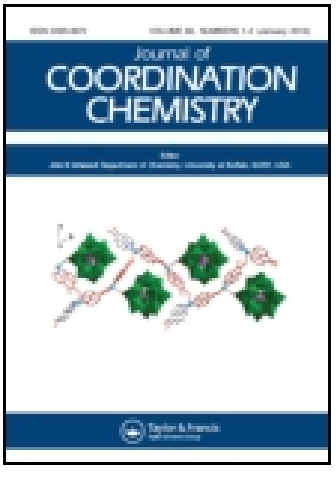

Journal of Coordination Chemistry
Publication details, including instructions for authors and subscription information:
http://www.tandfonline.com/loi/gcoo20

Supramolecular coexistence of Co(II) and Ag(I) complexes based on polyoxotungstate and imidazoles: synthesis, crystal structure, and spectroscopic study

Wei Wang[a], Yunfeng Qiu[a] & Lin Xu[a]
[a] Key Laboratory of Polyoxometalates Science of Ministry of Education, College of Chemistry, Northeast Normal University, Changchun, PR China

Accepted author version posted online: 25 Mar 2014.Published online: 22 Apr 2014.

To cite this article: Wei Wang, Yunfeng Qiu & Lin Xu (2014) Supramolecular coexistence of Co(II) and Ag(I) complexes based on polyoxotungstate and imidazoles: synthesis, crystal structure, and spectroscopic study, Journal of Coordination Chemistry, 67:5, 797-806, DOI: 10.1080/00958972.2014.908464

To link to this article: http://dx.doi.org/10.1080/00958972.2014.908464

Journal of Coordination Chemistry, 2014
Vol. 67, No. 5, 797–806, http://dx.doi.org/10.1080/00958972.2014.908464

Supramolecular coexistence of Co(II) and Ag(I) complexes based on polyoxotungstate and imidazoles: synthesis, crystal structure, and spectroscopic study

WEI WANG, YUNFENG QIU and LIN XU*

Key Laboratory of Polyoxometalates Science of Ministry of Education, College of Chemistry, Northeast Normal University, Changchun, PR China

(*Received 21 November 2013; accepted 26 February 2014*)

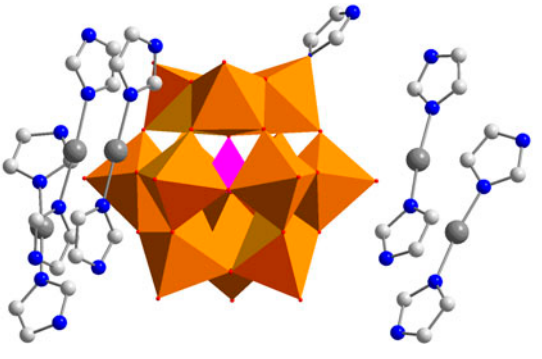

In this work, $[Ag(imi)_2]_5[PW_{11}O_{39}Co(imi)]\cdot 2.5H_2O$ (**1**, imi = imidazole) based on both polyoxometalate and imidazole has been synthesized by using the hydrothermal method. Its structure and spectroscopic properties were determined by single-crystal X-ray diffraction, elemental analysis, IR spectrum, diffuse reflectance UV–Vis spectrum, and thermogravimetric analysis. Single-crystal X-ray diffraction analysis indicates that **1** is a 3-D supramolecular interpenetrating structure, constructed from $[Co(imi)]^{2+}$ monosubstituted Keggin-type heteropolytungstate and $\{[Ag(imi)_2]^+\}_5$ complexes. Imidazole ligands play dual roles in **1**, both coordination linker and supermolecule linker. The luminescence spectrum of **1** displays a strong emission peak at 469 nm excited at 208 nm. Coexistence of Co(II) and Ag(I) complexes with 3-D supramolecular architecture may find application in photoluminescent materials and catalysis.

Keywords: Polyoxometalates; Imidazole; Transition metal; Luminescence

1. Introduction

Coordination assembly of transition metal complexes based on polyoxometalates (POMs) is a hot topic in coordination chemistry, ascribed to the applications in catalysis, magnetism,

*Corresponding author. Email: linxu@nenu.edu.cn

drugs, fluorescence, absorption, and many other fields [1–8]. Substituted polyoxoanions are excellent building blocks in the functional POMs field because they possess higher negative charges than saturated type Keggin polyoxoanions, which activates the surface oxygens of polyanions, and coordinates with other bridges to realize the functionalization [9–13]. In POM-based organic supermolecules, there are hydrogen bonds, π–π packing, or electrostatic interactions, which provide new functions to POMs. There are many supermolecular compounds constructed from saturated and vacant POMs [14–17], but supramolecular compounds based on functionalized polyoxoanions are rare [18]. This is attributed to the larger volume of the functional polyoxoanions and the larger steric effect among metal-organic frameworks may bring difficulties to the synthesis. Particularly, the use of inorganic POM and organic imidazole to assemble new transition metal complexes should be of interest to coordination chemistry and materials science. Here, we report a new complex $[Ag(imi)_2]_5[PW_{11}O_{39}Co(imi)]\cdot 2.5H_2O$ (**1**), which has been synthesized by the hydrothermal method and characterized by single-crystal X-ray diffraction, elemental analysis, IR, TG, diffuse reflectance UV–Vis spectra, and TG analyses; the luminescence of **1** has also been investigated, demonstrating that **1** may be a potential photoluminescent material.

2. Experimental setup

2.1. *Materials and physical measurements*

All chemicals were commercially purchased and used without purification. FT-IR spectra were recorded from 400 to 4000 cm^{-1} on an Alpha Centaurt FT-IR spectrophotometer using KBr pellets. Elemental analyses of P, W, Co, and Ag were performed by a Leaman inductively coupled plasma spectrometer; C, H, and N were performed on a Perkin-Elmer 2400 CHN elemental analyzer. TG analyses were performed on a Perkin-Elmer TGA7 instrument in flowing N_2 with a heating rate of 10 °C min^{-1}. Diffuse reflectance UV–Vis spectrum for **1** ($BaSO_4$ pellet) was obtained with a Varian Cary 500 UV–Vis NIR spectrometer. Luminescence spectrum for solid sample was recorded with a FL-2T2 (SPEX, USA) fluorescence spectrophotometer.

2.2. *Synthesis of 1*

A mixture of $Na_2WO_4\cdot 2H_2O$, H_3PO_4, $CoCl_2\cdot 6H_2O$, $AgNO_3$, imi, and H_2O with the molar ratio of 5 : 1 : 2 : 2 : 2 : 500 was stirred for 30 min in air. The mixture was then transferred to a Teflon-lined autoclave (23 mL) and kept at 160 °C for four days. After the autoclave was slowly cooled to room temperature at 10 °C h^{-1} and crystallized for two days, pink crystals were filtered off, washed with distilled water, and then dried in a desiccator at room temperature (yield 72% based on W). Elemental analysis for $C_{33}H_{38}Ag_5CoN_{22}O_{41.5}PW_{11}$ (**1**): Calcd C, 9.77; H, 0.94; N, 7.60; P, 0.76; Co, 1.45; Ag, 13.29; W, 49.83 (%). Found: C, 9.71; H, 1.22; N, 7.53; P, 0.71; Co, 1.40; Ag, 13.19, W, 49.11 (%).

2.3. *Crystal structure determination*

Single crystals of **1** of 0.22 × 0.20 × 0.15 mm were mounted on glass fibers. The crystallographic data were collected at 293 K for **1** on a Rigaku R-axis Rapid IP diffractometer using

graphite-monochromated Mo Kα radiation ($\lambda = 0.71073$ Å) operating at 50 kV and 200 mA with IP technique. Data processing was accomplished with the RAXWISH processing program. Empirical absorption correction was applied. The structure of **1** was solved by the

Table 1. The crystal data and structure refinement for **1**.

Empirical formula	$C_{33}H_{38}Ag_5CoN_{22}O_{41.5}PW_{11}$
M	4058.34
Crystal system	Triclinic
Space group	*P1*
a (Å)	12.801(3)
b (Å)	13.180(3)
c (Å)	13.490(3)
α (°)	68.18(3)
β (°)	85.66(3)
γ (°)	66.39(3)
V (Å$^{3)}$	1928.9(8)
Z	1
D_{Calcd} (mg m^{-3})	3.494
μ (mm^{-1})	17.886
F (0 0 0)	1812
θ Range (°)	3.09–25.00
Data/restraints/parameters	15,163/11,386
R_{int}	0.0440
$R_1(I > 2\sigma(I))$[a]	0.0502
wR_2[a]	0.1243
Goodness-of-fit on F^2	1.064
$\Delta\rho_{max,\ min}$/e Å^{-3}	1.834, –2.108

[a]$R_1 = \sum||F_0| - |F_C||/\sum|F_0|$; $wR_2 = \sum[w(F_0^2 - F_C^2)^2]/\sum[w(F_0^2)^2]^{1/2}$.

Table 2. Selected bond lengths for **1**.

W(1)–O(1)	1.67(2)	W(5)–O(39)	2.540(14)	W(10)–O(32)	1.95(2)
W(1)–O(13)	1.77(2)	W(6)–O(6)	1.66(3)	W(10)–O(40)	2.46(2)
W(1)–O(20)	1.90(2)	W(6)–O(28)	1.82(3)	W(11)–O(11)	1.644(19)
W(1)–O(12)	1.92(3)	W(6)–O(31)	1.854(19)	W(11)–O(23)	1.84(2)
W(1)–O(14)	1.97(2)	W(6)–O(30)	1.90(2)	W(11)–O(34)	1.91(2)
W(1)–O(38)	2.488(13)	W(6)–O(29)	1.91(3)	W(11)–O(21)	1.94(2)
W(2)–O(2)	1.72(2)	W(6)–O(39)	2.474(18)	W(11)–O(33)	1.99(3)
W(2)–O(18)	1.84(2)	W(7)–O(7)	1.70(3)	W(11)–O(37)	2.481(16)
W(2)–O(15)	1.88(2)	W(7)–O(32)	1.87(2)	P(1)–O(39)	1.483(17)
W(2)–O(16)	1.91(3)	W(7)–O(31)	1.896(18)	P(1)–O(37)	1.504(17)
W(2)–O(17)	1.98(2)	W(7)–O(33)	1.91(2)	P(1)–O(38)	1.519(19)
W(2)–O(40)	2.408(15)	W(7)–O(22)	1.95(3)	P(1)–O(40)	1.54(2)
W(3)–O(3)	1.70(3)	W(7)–O(37)	2.481(16)	Co(1)–O(13)	1.96(2)
W(3)–O(17)	1.843(19)	W(8)–O(8)	1.650(19)	Co(1)–O(27)	2.02(3)
W(3)–O(19)	1.89(3)	W(8)–O(24)	1.82(3)	Co(1)–O(18)	2.05(2)
W(3)–O(22)	1.89(2)	W(8)–O(34)	1.86(2)	Co(1)–O(35)	2.08(2)
W(3)–O(21)	1.94(2)	W(8)–O(29)	1.92(3)	Co(1)–N(1)	2.089(18)
W(3)–O(37)	2.444(14)	W(8)–O(26)	1.94(2)	Co(1)–O(40)	2.378(17)
W(4)–O(4)	1.67(2)	W(8)–O(39)	2.517(15)	Ag(1)–N(3)	2.07(2)
W(4)–O(23)	1.88(2)	W(9)–O(9)	1.68(3)	Ag(1)–N(5)	2.17(2)
W(4)–O(24)	1.92(3)	W(9)–O(14)	1.92(2)	Ag(2)–N(9)	2.09(2)
W(4)–O(12)	1.96(3)	W(9)–O(15)	1.92(2)	Ag(2)–N(7)	2.19(2)
W(4)–O(25)	2.01(2)	W(9)–O(25)	1.93(2)	Ag(3)–N(15)	2.03(2)
W(4)–O(38)	2.537(15)	W(9)–O(19)	1.93(2)	Ag(3)–N(13)	2.09(2)
W(5)–O(5)	1.685(19)	W(9)–O(38)	2.436(15)	Ag(4)–N(21)	2.01(3)
W(5)–O(27)	1.71(3)	W(10)–O(10)	1.72(2)	Ag(4)–N(11)	2.05(3)
W(5)–O(20)	1.88(3)	W(10)–O(35)	1.86(2)	Ag(5)–N(19)	2.02(3)
W(5)–O(28)	1.92(3)	W(10)–O(30)	1.889(19)	Ag(5)–N(17)	2.08(3)
W(5)–O(26)	1.98(2)	W(10)–O(16)	1.90(2)		

Table 3. Selected bond angles for **1**.

O(1)–W(1)–O(13)	106.8(11)	O(5)–W(5)–O(26)	92.8(10)	O(10)–W(10)–O(30)	104.7(11)
O(1)–W(1)–O(20)	103.4(11)	O(5)–W(5)–O(39)	156.9(9)	O(10)–W(10)–O(16)	101.5(11)
O(1)–W(1)–O(12)	93.9(12)	O(6)–W(6)–O(28)	103.2(14)	O(10)–W(10)–O(32)	99.9(10)
O(1)–W(1)–O(14)	97.9(11)	O(6)–W(6)–O(31)	105.2(12)	O(10)–W(10)–O(40)	167.6(8)
O(1)–W(1)–O(38)	158.4(10)	O(6)–W(6)–O(30)	106.6(14)	O(11)–W(11)–O(23)	108.3(12)
O(2)–W(2)–O(18)	101.6(10)	O(6)–W(6)–O(29)	97.7(14)	O(11)–W(11)–O(34)	103.3(10)
O(2)–W(2)–O(15)	100.8(14)	O(6)–W(6)–O(39)	162.1(11)	O(11)–W(11)–O(21)	101.4(10)
O(2)–W(2)–O(16)	102.8(14)	O(7)–W(7)–O(32)	106.2(13)	O(11)–W(11)–O(33)	98.3(11)
O(2)–W(2)–O(17)	97.7(10)	O(7)–W(7)–O(31)	104.2(11)	O(11)–W(11)–O(37)	163.6(8)
O(2)–W(2)–O(40)	170.1(13)	O(7)–W(7)–O(33)	97.7(13)	O(39)–P(1)–O(37)	111.1(10)
O(3)–W(3)–O(17)	109.9(12)	O(7)–W(7)–O(22)	100.6(12)	O(39)–P(1)–O(38)	108.4(11)
O(3)–W(3)–O(19)	101.3(14)	O(7)–W(7)–O(37)	163.1(11)	O(39)–P(1)–O(40)	111.5(12)
O(3)–W(3)–O(22)	98.7(14)	O(8)–W(8)–O(24)	106.0(13)	O(13)–Co(1)–O(27)	88.6(10)
O(3)–W(3)–O(21)	94.4(13)	O(8)–W(8)–O(34)	106.6(11)	O(13)–Co(1)–O(18)	90.3(9)
O(3)–W(3)–O(37)	159.2(11)	O(8)–W(8)–O(29)	101.4(12)	O(13)–Co(1)–O(35)	165.5(9)
O(4)–W(4)–O(23)	103.8(10)	O(8)–W(8)–O(26)	100.0(10)	O(13)–Co(1)–N(1)	100.1(8)
O(4)–W(4)–O(24)	106.5(12)	O(8)–W(8)–O(39)	164.2(10)	O(13)–Co(1)–O(40)	91.6(8)
O(4)–W(4)–O(12)	106.0(11)	O(9)–W(9)–O(14)	97.6(13)	N(3)–Ag(1)–N(5)	175.1(10)
O(4)–W(4)–O(25)	99.1(11)	O(9)–W(9)–O(15)	101.1(13)	N(9)–Ag(2)–N(7)	174.1(10)
O(4)–W(4)–O(38)	166.4(9)	O(9)–W(9)–O(25)	98.4(13)	N(15)–Ag(3)–N(13)	168.7(11)
O(5)–W(5)–O(27)	107.2(12)	O(9)–W(9)–O(19)	100.2(13)	N(21)–Ag(4)–N(11)	176.5(15)
O(5)–W(5)–O(20)	103.6(11)	O(9)–W(9)–O(38)	164.5(11)	N(19)–Ag(5)–N(17)	173.3(12)
O(5)–W(5)–O(28)	104.7(12)	O(10)–W(10)–O(35)	99.8(9)		

direct method and refined by the full-matrix least squares on F^2 using the SHELXTL-97 crystallographic software package. A total of 15,163 reflections for **1** were collected, of which 11,386 reflections were unique. During the refinement of **1**, anisotropic thermal parameters were used to refine all non-hydrogen atoms; $R_1 = 0.0502$, $wR_2 = 0.1243$. The crystal data and structure refinement for **1** are listed in table 1 and selected bond lengths for **1** are listed in table 2. Selected bond angles for **1** are listed in table 3.

3. Results and discussion

3.1. *Description of the crystal structures*

Single-crystal X-ray diffraction analysis shows that **1** is composed of a functionalized polyoxoanion $[PW_{11}O_{39}Co(imi)]^{5-}$, five $[Ag(imi)_2]^+$ cations, and $2.5H_2O$. Figure 1 is the structure of **1**, $[PW_{11}O_{39}Co(imi)]^{5-}$ consists of a $[Co(imi)]^{2+}$ and a monovacant $[PW_{11}O_{39}]^{7-}$. $[PW_{11}O_{39}]^{7-}$ is a monovacant α-Keggin structure, which is constructed from 11 $\{WO_6\}$ octahedra and a $\{PO_4\}$ tetrahedron; all the W centers display octahedral coordination geometry. The central P is four-coordinate. $[Co(imi)]^{2+}$ coordinates to the vacant position of $[PW_{11}O_{39}]^{7-}$, realizing the functionalization of the monovacant Keggin-type polyoxoanion. The W–O bond lengths are 1.650(19)–2.540(14) Å and O–W–O angles are 92.8(10)°–170.1(13)°; P–O bond lengths are 1.483(17)–1.54(2) Å and O–P–O angles vary from 108.4(11)° to 111.5(12)°; Co–O bond lengths are 1.96(2)–2.378(17) Å and O–Co–O angles are 88.6(10)°–165.5(9)°; Co–N bond length is 2.089(18) Å and O–Co–N angle is 100.1(8)°. Bond valence sum calculation [19] indicates that the oxidation states of W, P, and Co are +6, +5, and +2. There are five $[Ag(imi)_2]^+$ cations around the functionalized polyoxoanions, each constructed from a Ag^+ and two imi molecules. Ag is two-coordinate, with linear geometry. Ag–N bond lengths are 2.01(3)–2.19(2) Å and N–Ag–N angles are 168.7(11)°–176.5(15)°. Bond valence sum calculation indicates that the oxidation state of all silvers is +1 [19].

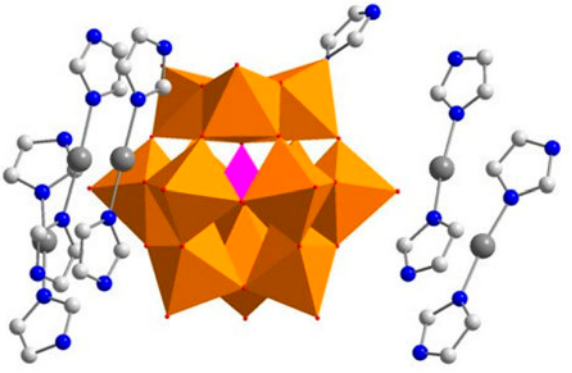

Figure 1. The structure of **1**. The water molecules, hydrogens, and hydrogen bonds are omitted for clarity. {WO_6}, orange polyhedra; {PO_4}, pink polyhedron; C, light gray; N, blue; Ag, deep gray (see http://dx.doi.org/10.1080/00958972.2014.908464 for color version).

$[Ag(imi)_2]^+$ cations are connected through π–π packing interactions to form a 3-D supermolecular framework. Figure 2 shows π–π stacking representation of $[Ag(imi)_2]^+$ cations along the *b* axis; in the packing structure, the distance of adjacent imidazole rings is 3.420–3.634 Å. $[PW_{11}O_{39}Co(imi)]^{5-}$ polyoxoanions are connected through weak C–H···O interactions along the *b* axis to form the $[PW_{11}O_{39}Co(imi)]_n^{5n-}$ 1-D line, which inserts into the supermolecule structure based on $[Ag(imi)_2]^+$ cations. Figure 3 is the 3-D packing structure of **1** viewed along the *b* axis. Figure 4 is the schematic representation of the penetrating structure in **1**.

3.2. *Synthesis*

Synthesis of **1** was carried out under hydrothermal condition. It is important to control the proportion of reactants, the temperature of reaction, and the process of crystallization during

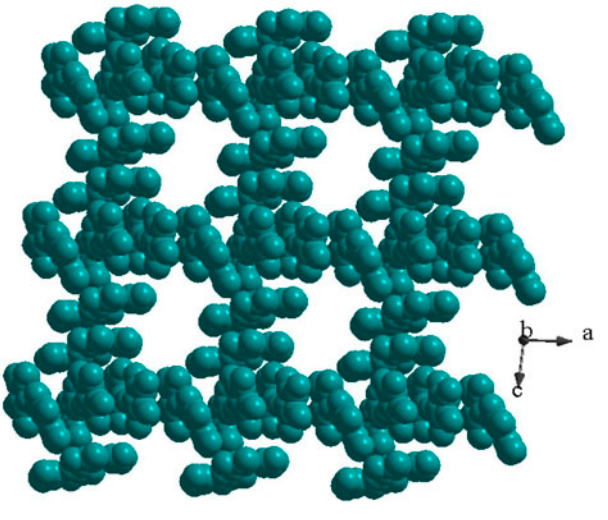

Figure 2. π–π stacking representation of $[Ag(imi)_2]^+$ cations in **1** along the *b* axis.

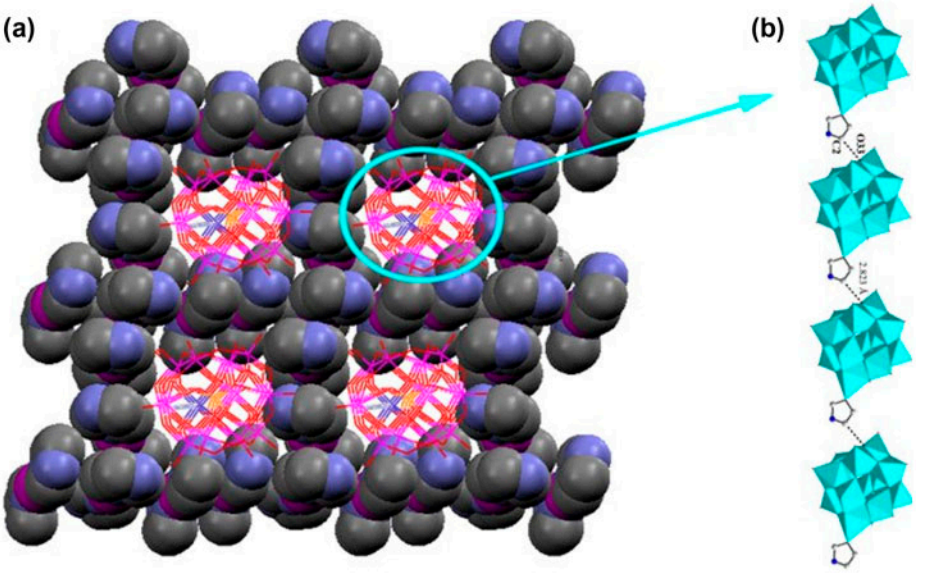

Figure 3. (a) The 3-D packing structure of **1** viewed along the *b* axis. (b) The 1-D structure of $[PW_{11}O_{39}Co(imi)]_n^{5n-}$ chains embedded in the channels. All hydrogens and waters are omitted for clarity.

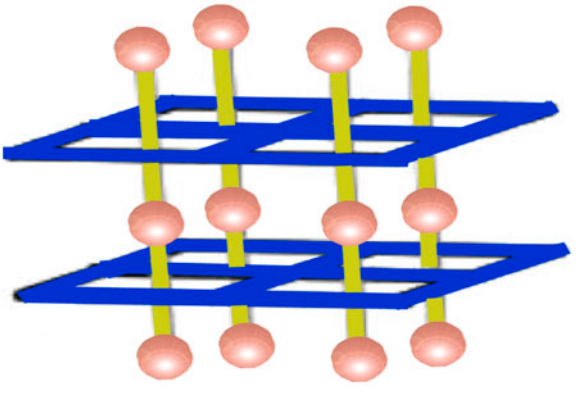

Figure 4. The schematic representation of the penetrating structure in **1**. The balls represent $[PW_{11}O_{39}Co(imi)]^{5-}$ polyoxoanions, the yellow sticks represent hydrogen bonds and blue grids represent π–π stacking structure of the $[Ag(imi)_2]^+$ cations (see http://dx.doi.org/10.1080/00958972.2014.908464 for color version).

the synthesis. The mole ratio of $Na_2WO_4{\cdot}2H_2O$, H_3PO_4, $CoCl_2{\cdot}6H_2O$, $AgNO_3$, imi, and H_2O was 5 : 1 : 2 : 2 : 2 : 500. Without this proportion, the product was either the saturated $[PW_{12}O_{40}]^{3-}$ or Co-substituted Keggin-type heteropolyanion. The reaction temperature was 160 °C; if the reaction temperature was higher or lower, different products with brown or black color could appear from the reaction. Crystals of **1** were crystallized for two days. In order to obtain high-quality crystals, crystallization is important. Without this time, the single-crystal products were small and without regular geometric structures.

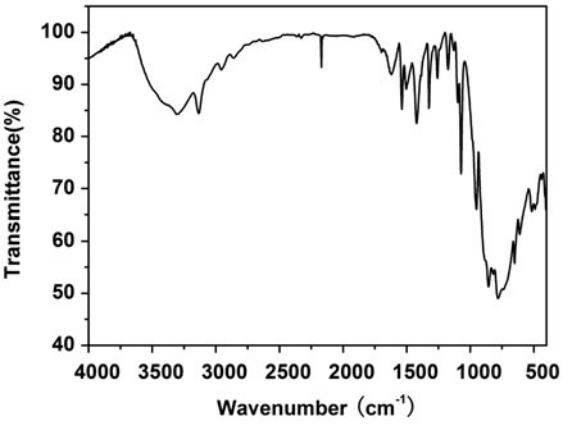

Figure 5. The IR spectrum of **1**.

3.3. *IR spectrum*

The IR spectrum of **1** (figure 5) shows peaks at 3308 and 3127 cm^{-1}, which are attributed to lattice water. Peaks at 3000–1100 cm^{-1} (2166, 1620, 1537, 1504, 1421, 1325, 1257, and 1174 cm^{-1}) are ascribed to imidazole. The peaks at 1098 and 1072 cm^{-1} are assigned to ν(P–O) vibrations. Compared to peak positions of saturated $[PW_{12}O_{40}]^{3-}$ [2], there exist position displacement and splitting in **1**, ascribed to the lower coordination symmetry resulting from $[Co(imi)]^{2+}$ coordinated monovacant Keggin polyoxoanion. Peaks at 952, 856, 819, and 781 cm^{-1} are assigned to vibrations of ν(W–O_c–W), ν(W–O_b–W), and ν(W–O_d), respectively.

3.4. *Thermogravimetric (TG) analysis*

In order to check the thermostability of **1**, the thermogravimetric (TG) measurement of **1** was carried out. As shown in figure 6, TG curve of **1** exhibits three weight losses. The total

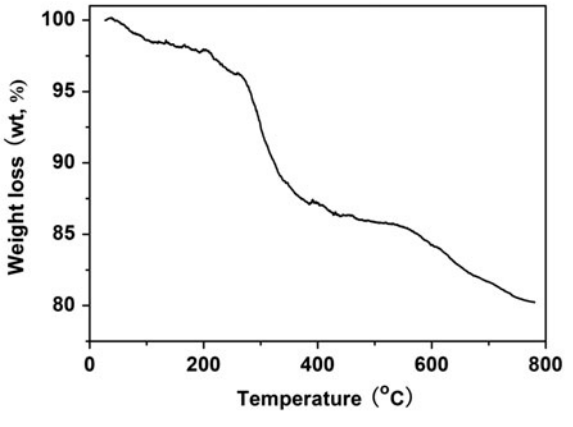

Figure 6. TG curve of **1**.

weight loss is 19.4 (weight loss is 19.3). The first weight loss from 50 to 130 °C resulted from loss of 2.5 crystalline waters. The second weight loss from 130 to 510 °C was ascribed to the decomposition of coordinated imidazole in $[Ag(imi)_2]^+$ and the resulting lattice waters. The third from 510 to 800 °C is assigned to the loss of residual imidazole in $[Co(imi)]^{2+}$ and $[Ag(imi)_2]^+$, together with the decomposition of polyoxotungstate anion.

3.5. *Diffuse reflectance UV–Vis spectra*

The diffuse reflectance UV–Vis spectra of **1** were investigated with solid-state samples in $BaSO_4$ pellets (figure 7). There is a strong absorption at 255 nm, attributed to O→W LMCT band [20]. The peak centered at 550 nm is ascribed to N/O→Co LMCT, which indicates strong interactions between imidazole molecules and polyoxoanions.

3.6. *Electrochemical investigation*

Because **1** is not soluble in aqueous solution, we use **1**-modified carbon paste electrode (**1**-CPE) to investigate its electrochemistry by measuring the cyclic voltammograms of **1**-CPE in 1 M H_2SO_4 solution at 10 mV s^{-1} (**1**-CPE was prepared by literature method [21]). As shown in figure S1 (see online supplemental material at http://dx.doi.org/10.1080/00958972.2014.908464), two quasi-reversible two-electron waves at cathodic potentials of −202 and −393 mV correspond to the tungsten-redox process. The anodic potential at +152 mV is ascribed to the oxidation of Co(II). The electrochemical behavior of **1**-CPE is similar to the reported for $[PFeW_{11}O_{39}]^{4-}$ at a modified carbon paste electrode in acidic medium [22]. These results indicate that the substituent transition metal ion (Co(II) or Fe(III)) has clear influence on the redox potentials of tungsten ions.

3.7. *Luminescent property*

The emission spectrum of **1** in the solid state at room temperature was investigated (figure 8). Upon light excitation at ca. 208 nm, the light emission of **1** at ca. 469 nm was observed. The emission is assigned to mixed ligand-to-ligand charge transfer and/or metal–metal–ligand

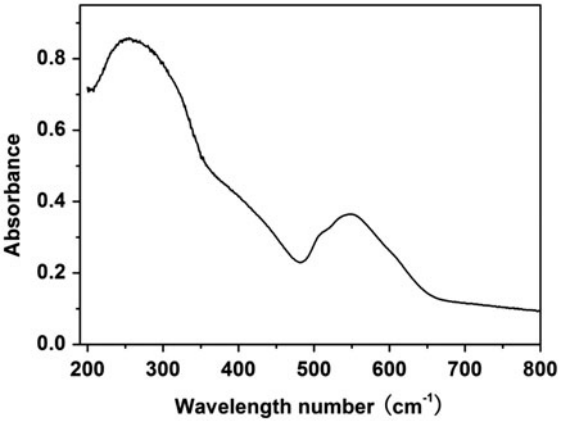

Figure 7. The diffuse reflectance UV–Vis spectrum of **1** in the solid state.

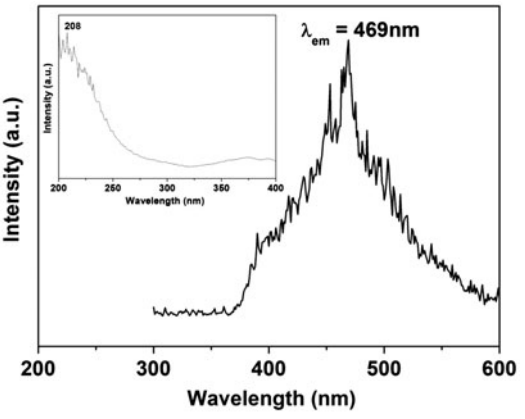

Figure 8. Excitation and emission spectra of **1** at room temperature.

charge transfer, which is due to the strong π–π interactions and weak Ag…Ag interactions in **1** [23]. Thus, there is energy transfer in internal molecules between metal and ligands. The investigation indicates that **1** is a potential photoluminescent material.

4. Conclusion

We obtained a new POMs-based supramolecular structure using hydrothermal method, with a 1-D $[PW_{11}O_{39}Co(imi)]_n^{5n-}$ inserted into the $[Ag(imi)_2]^+$-based supermolecular structure. Luminescence of **1** was due to the strong π–π interactions and weak Ag…Ag interactions in **1**. Cobalt(II) ion coordination with $XW_{11}O_{39}$ (X = P, Si, As, Ge) is easier with $XMo_{11}O_{39}$ complexes; this may be because the $XMo_{11}O_{39}$ unit is generally unstable in aqueous solution. The first $[PMo_{11}O_{39}Co]^{5-}$ complex was synthesized in acetonitrile [24], while the cesium salt of $[PMo_{11}O_{39}Co]^{5-}$ complex was also obtained from a one-pot synthesis [25]. Combination of $[PW_{11}O_{39}Co]^{5-}$ with organic component to form organic–inorganic hybrid could be used as catalysts in oxidation of various alcohols with hydrogen peroxide in acetonitrile [26]. In the future, our main research project is to synthesize the POM-based materials using other polydentate long chain ligands in order to obtain the POMs with new functional properties.

Supplementary material

CCDC 971272 contains the supplementary crystallographic data of **1,** in which the full bond lengths and angles are supplied. The detailed data of electrochemical and powder X-ray diffraction measurements are presented in the Supporting Information. The data can be obtained free of charge from The Cambridge Crystallographic Data Center via www.ccdc.cam.ac.uk/data_request/cif.

Funding

This project is financially supported by the Natural Science Foundation of China [grant number 21001021], [grant number 21273031].

References

[1] M.T. Pope, A. Müller. *Angew. Chem. Int. Ed. Engl.*, **30**, 34 (1991).
[2] D.L. Long, R. Tsunashima, L. Cronin. *Angew. Chem. Int. Ed.*, **49**, 1736 (2010).
[3] U. Kortz, F. Hussain, M. Reicke. *Angew. Chem. Int. Ed.*, **44**, 3773 (2005).
[4] A. Proust, R. Thouvenot, P. Gouzerh. *Chem. Commun.*, **44**, 1873 (2008).
[5] H. Lv, Y.V. Geletii, C. Zhao, J.W. Vickers, G. Zhu, Z. Luo, J. Song, T. Lian, D.G. Musaev, C.L. Hill. *Chem. Soc. Rev.*, **41**, 7572 (2012).
[6] O. Oms, A. Dolbecq, P. Mialane. *Chem. Soc. Rev.*, **41**, 7497 (2012).
[7] G. Gao, F. Li, L. Xu, X. Liu, Y. Yang. *J. Am. Chem. Soc.*, **130**, 10838 (2008).
[8] F. Li, L. Xu. *Dalton Trans.*, 4024 (2011).
[9] X.L. Wang, H.Y. Lin, Y.F. Bi, B.K. Chen, G.C. Liu. *J. Solid State Chem.*, **181**, 556 (2008).
[10] J.Y. Niu, M.L. Wei, J.P. Wang, D.B. Dang. *Eur. J. Inorg. Chem.*, 160 (2004).
[11] J.R. Galán-Mascarós, C. Giménez-Saiz, S. Triki, C.J. Gómez-García, E. Coronado, L. Ouahab. *Angew. Chem. Int. Ed. Engl.*, **34**, 1460 (1995).
[12] J.Y. Kim, S.M. Park, H. So. *Bull. Korean Chem. Soc.*, **18**, 369 (1997).
[13] D.E. Katsoulis, M.T. Pope. *J. Chem. Soc., Dalton Trans.*, 1483 (1989).
[14] A.X. Tian, J. Ying, J. Peng. *Inorg. Chem.*, **48**, 100 (2009).
[15] H. Liu, L. Xu, G.G. Gao, F.Y. Li, Y.Y. Yang, Z.K. Li, Y. Sun. *J. Solid State Chem.*, **180**, 1664 (2007).
[16] C.Y. Sun, S.X. Liu, D.D. Liang, K.Z. Shao, Y.H. Ren, Z.M. Su. *J. Am. Chem. Soc.*, **131**, 1883 (2009).
[17] S. Reinoso, P. Vitoria, J.M. Gutiérrez-Zorrilla, L. Lezama, L. San Felices, J.I. Beitia. *Inorg. Chem.*, **44**, 9731 (2005).
[18] C. Dablemont, A. Proust, R. Thouvenot, C. Afonso, F. Fournier, J.C. Tabet. *Inorg. Chem.*, **43**, 3514 (2004).
[19] I.D. Brown, D. Altermatt. *Acta Crystallogr. B*, **41**, 244 (1985).
[20] W.L. Chen, B.W. Chen, Y.G. Li, Y.H. Wang, E.B. Wang. *Inorg. Chim. Acta*, **362**, 5043 (2009).
[21] C. Qin, X.L. Wang, E.B. Wang, Z.M. Su. *Inorg. Chem.*, **47**, 5555 (2008).
[22] H. Hamidi, E. Shams, B. Yadollahi, F. Kabiri Esfahani. *Electrochim. Acta*, **54**, 3495 (2009).
[23] J. Lü, F.X. Xiao, L.X. Shi, R. Cao. *J. Solid State Chem.*, **181**, 313 (2008).
[24] L.A. Combs-Walker, C.L. Hill. *Inorg. Chem.*, **30**, 4016 (1991).
[25] A. Patel, S. Pathan. *J. Coord. Chem.*, **65**, 3122 (2012).
[26] Z. Nadealian, V. Mirkhani, B. Yadollahi, M. Moghadam, S. Tangestaninejad, I. Mohammadpoor-Baltork. *J. Coord. Chem.*, **65**, 1071 (2012).